Plant Physiol. (1997) 115: 949–957

Starches from A to C[1]

Chlamydomonas reinhardtii as a Model Microbial System to Investigate the Biosynthesis of the Plant Amylopectin Crystal

Alain Buléon, Daniel J. Gallant, Brigitte Bouchet, Gregory Mouille, Christophe D'Hulst, Jens Kossmann, and Steven Ball*

Institut National de la Recherche Agronomique, Centre de Recherches Agroalimentaires, Rue de la Géraudière, B.P. 71627, 44316 Nantes Cedex 03, France (A.B., D.J.G., B.B.); Laboratoire de Chimie Biologique, Unité Mixte de Recherche du Centre National de la Recherche Scientifique no. 111, Université des Sciences et Technologies de Lille, 59655 Villeneuve d'Ascq Cedex France (G.M., C.D., S.B.); and Max-Planck-Institut für Molekulare Pflanzenphysiologie, 14476 Golm, Germany (J.K.)

Wide-angle powder x-ray diffraction analysis was carried out on starch extracted from wild-type and mutant *Chlamydomonas reinhardtii* cells. Strains containing no defective starch synthases as well as mutants carrying a disrupted granule-bound starch synthase structural gene displayed the A type of diffraction pattern with a high degree of crystallinity. Mutants carrying a defect for the major soluble starch synthase (SSS), SSS II, were characterized by a switch to the B type of diffraction pattern with very low crystallinity. Mutant strains carrying SSS I as the only glucan elongation enzyme regained some of their crystallinity but switched to the C type of diffraction pattern. Differential scanning calorimetry analysis correlated tightly with the x-ray diffraction results. Together with the electron microscopy analyses, these results establish *C. reinhardtii* as a microbial model system displaying all aspects of cereal starch synthesis and structure. We further show that SSS II is the major enzyme involved in the synthesis of crystalline structures in starch and demonstrate that SSS I alone builds a new type of amylopectin structure.

Starch is by far the major storage compound accumulated by plants, making it one of the most abundant polysaccharides present on earth. Above all, it remains the most important source of calories in the human and animal diet and has also become a major source of plant raw material for nonfood purposes. Over 600 different commercial products are generated by the starch extraction and processing industry.

In contrast to its economic importance, our understanding of starch biosynthesis is limited to the extent that further genetic improvements are dependent on additional understanding of how the final structure is built. Microbial genetics has until very recently been of little help in understanding how the complex granule structure is built (for reviews, see Müller-Röber and Kossmann, 1994; Ball et al., 1996; Preiss and Sivak, 1996; Smith et al., 1997). This is mainly because starch accumulates only in photosynthetic eukaryotes, whereas model microorganisms such as bacteria or yeasts synthesize glycogen as a far less organized form of storage polysaccharide. Yet, as shown by the relatedness in primary structure of many enzymes in the pathway, there is little doubt that starch metabolism has emerged in the chloroplast from the preexisting cyanobacterial glycogen pathway.

Because the glycogen-accumulating cyanobacteria are not useful in explaining the building of the crystalline structures present in starch granules, we have recently established *Chlamydomonas reinhardtii*, a unicellular eukaryotic green alga of the order Volvocales, as a suitable model microorganism with which to investigate the genetics of plant starch biosynthesis. Studies in *C. reinhardtii* have indeed helped to ascertain the in vivo function of many of the starch biosynthetic enzymes (Ball et al., 1991; Delrue et al., 1992; Fontaine et al., 1993; Maddelein et al., 1994; Mouille et al., 1996; Van den Koornhuyse et al., 1996). Among these, mutants defective for two out of the three ADP-Glc α-1,4-glucan α-4-glucosyltransferases, known as starch synthases, have been selected (Delrue et al., 1992; Fontaine et al., 1993). Mutants with a defect in the one of the two SSSs (SSSII) witness a major defect in the synthesis of amylopectin. The remaining polysaccharide displays a large decrease in chains, the lengths of which range between 10 and 40 Glc residues and a relative increase of very short chains with a clear maximum of chains of 6 Glc residues. Mutants in the major GBSS are characterized by

[1] This work was supported by grants from the Ministère de l'Education Nationale, the Ministère de l'Agriculture, the Institut National de la Recherche Agronomique, the Centre National de la Recherche Scientifique (Unité Mixte de Recherche du Centre National de la Recherche Scientifique no. 111, Director André Verbert), the Max-Planck-Institut für Molekulare Pflanzenphysiologie, and the European Union, FAIR grant no. CT95-0568.

* Corresponding author; e-mail steven.ball@univ-lille1.fr; fax 33-3-20-43-65-55.

Abbreviations: DP, degree of polymerization; DSC, differential scanning calorimetry; GBSS, granule-bound starch synthase; SSS, soluble starch synthase; T_e, temperature at the end of the endotherm; T_{max}, temperature at the endotherm maximum; T_o, temperature at the onset of the endotherm.

the disappearance of amylose, whereas modifications in the chain-length distribution of amylopectin are restricted to a decrease in the extra-long (above 50 Glc residues in length) chain fraction. Culture conditions could even be found that mimic the synthesis of plant leaf starch (transient starch) or that of storage starch occurring in the amyloplast (Ball et al., 1990; Libessart et al., 1995).

The evidence from biochemical studies that has accumulated over the years suggests that the structure of *C. reinhardtii* starch extracted from nitrogen-starved cultures could not be distinguished from that of maize endosperm storage starch, the major crop for both human nutrition and starch extraction. Plant starches are generally classified into three types (A, B, and C) according to the kind of x-ray diffraction pattern given by their amylopectin crystalline lattices. A-type starches can be found in cereal endosperms, whereas B and C types were reported for tubers and pea embryos, respectively (for review, see Imberty et al., 1991).

Three-dimensional structures involving parallel double helices have been published for both the A and B patterns (Fig. 1). It is suspected that the C type is due to a mix of both kinds of crystals in a single or distinct granule and that it does not define a structure of its own. The three-dimensional structures of these crystals are of paramount importance in determining most of the functional and industrial properties of starches. The generalization of the results obtained in *Chlamydomonas* sp. to higher plants requires that both build the same kind of polysaccharide secondary and tertiary structures.

In this paper we show that *C. reinhardtii* accumulates a storage polysaccharide of the A type, thereby affirming the analogy that was previously drawn with maize endosperm starch. As with higher plants, mutants lacking amylose because of a defect in the major GBSS display the very same three-dimensional arrangement of the amylopectin glucans. However, in the absence of SSSII the crystallinity collapses and switches to the B type. Starches built by mutants that lack both activities and that have thus retained SSSI as sole elongation enzyme have regained some crystallinity but gave the C type of x-ray diffraction pattern. We believe that these results establish a major function for SSSII in the building of the amylopectin crystalline lattice of the wild-type *C. reinhardtii* cell.

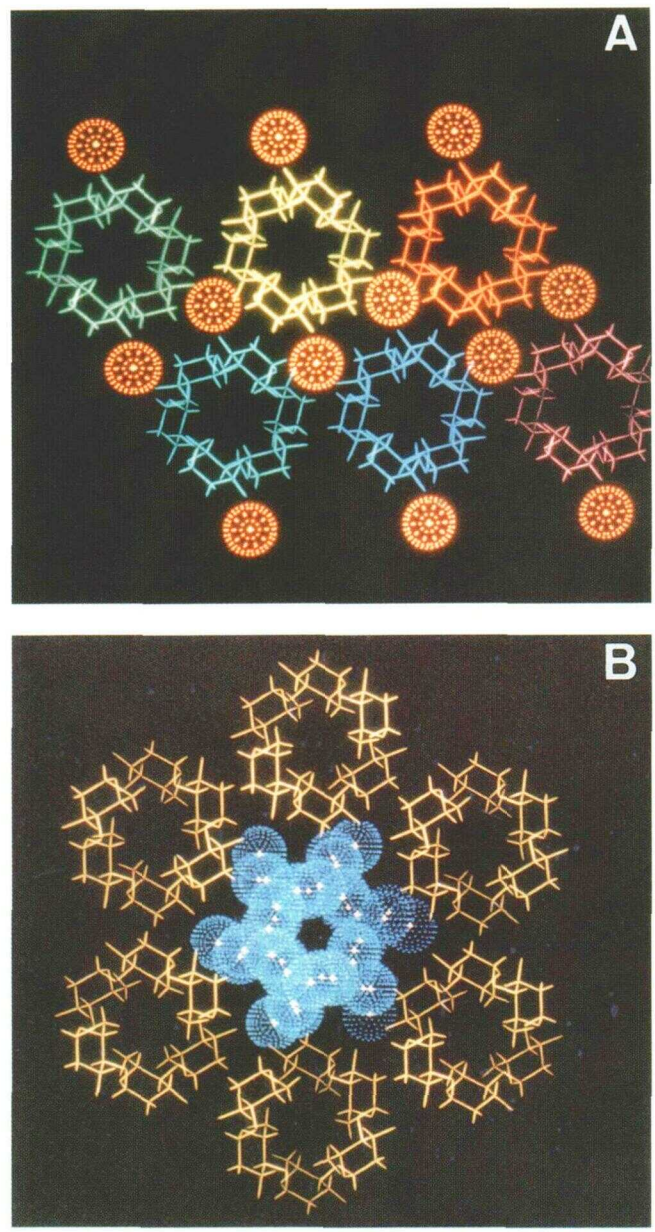

Figure 1. Three-dimensional representation of amylopectin crystalline structures. A, Cross-section of the A-type lattice of parallel glucan double helices after Imberty et al. (1988). The position of water molecules are displayed as orange spheres. B, Cross-section of the B-type lattice of parallel glucan double helices after Imberty and Perez (1988). Water molecules are displayed in blue.

MATERIALS AND METHODS

Materials

[U-^{14}C]ADP-Glc was purchased from Amersham. The starch determination kit was purchased from Boehringer Mannheim. Rabbit liver glycogen was supplied by Sigma. Percoll was from Pharmacia LKB Biotechnology (Uppsala, Sweden).

Strains, Media, Incubation, and Growth Conditions

Our reference strains are 137C, (*mt⁻ nit1 nit2*), I152 (*mt⁻ nit1 nit2 sta3–1*), BAFR1 (*mt⁺ nit1 nit2 arg7 cw15 sta2–29::ARG7*), and IJ2 (*mt⁻ sta2–29::ARG7 sta3–1*). Starch was always prepared from nitrogen-starved media. Media and culture conditions used in our starvation experiments were as described by Ball et al. (1990). Recipes for TAP and HSA media and genetic techniques can be found in Harris (1989a, 1989b). All experiments were performed under continuous light (40 μE m^{-2} s^{-1}) in the presence of acetate at 24°C in liquid cultures that were shaken vigorously without CO_2 bubbling.

Starch Purification

Pure native starch was prepared from nitrogen-limited (8 mg $L^{-1}[NH_4]_2SO_4$) cultures, inoculated at 10^5 cells mL^{-1}, and harvested after 5 d of growth under continuous light (40 $\mu E\ m^{-2}\ s^{-1}$) in otherwise HSA or TAP medium (Harris, 1989a, 1989b). Algae were ruptured by sonication at a density of 10^8 cells mL^{-1}. A crude starch pellet was obtained by spinning the lysate at 2000*g* for 20 min. The pellet was rinsed in 10 mM Tris HCl (pH 8.0) and 1 mM EDTA, resuspended in 1 mL of the same buffer per 10^8 starting cells, and passed twice through a Percoll gradient (9 mL of Percoll per milliliter of crude starch pellet). The purified starch pellet was rinsed by two centrifugations at 2000*g* in distilled water and was kept at 4°C for immediate use or was dried for subsequent analysis. Starch amounts were measured using the amyloglucosidase assay described in Delrue et al. (1992).

X-Ray Diffraction Measurements

Samples (5–20 mg) were sealed between two pieces of aluminum foil to prevent any significant change in water content during the measurement. Diffraction diagrams were recorded using x-ray equipment (Inel, Artenay, France) operating at 40 keV and 30 mA. CuK_α 1 radiation (λ=0.15405 nm) was selected using a quartz monochromator. A curved, position-sensitive detector (CPS120, Inel) was used to monitor the diffracted intensities using 2-h exposure periods. Relative crystallinity was determined after bringing all recorded diagrams at the same scale using normalization of the total scattering between 3 and 30° (2q), following a method derived from Murthy and Minor (1990). Dry extruded starch was used as the amorphous standard. The respective amounts of A and B types in starches presenting mixed diagrams were calculated using a multilinear regression, assuming that the experimental diagram is a linear combination of elementary diagrams of amorphous A and B types. Recrystallized amylose was used for A and B standards.

DSC

Samples (about 20 mg) were weighed in stainless steel high-pressure pans and about 80 μL of distilled water was added before sealing. An automated heat-flux differential scanning calorimeter (DSC 121, Setaram, Caluire, France) was used, and scans between 20 and 180°C were run at 3°C/min and ±40 mW full scale. Calibration was checked using indium (429.6 K) and gallium (302.7 K) melting. The reference cell contained 100 μL of water. Melting enthalpies were calculated with respect to dry matter, after water content determination, using subsequent drying at 50°C during one night and 130°C during 6 h.

Scanning Electron Microscopy

Dried starch granules were stuck onto brass stubs with double-sided carbon-conductive adhesive tape and covered with a 30-nm gold layer using a 1100-ion sputtering device (Jeol). The specimens were then examined with a 840A scanning electron microscope (Jeol) operating at an accelerating voltage of 5 keV with a current probe of 0.1 nA. The working distance was 15 mm.

Transmission Electron Microscopy

Samples were first embedded at 45°C in a 3% agar gel to prevent heterogeneous distribution and small, solidified cubes of agar-containing samples were cut (1 mm^3) (Gallant, 1974). The PATAg staining procedure for carbohydrates was used before resin embedding: the samples were first stained by immersion in a 1% periodic acid solution for 5 min, followed by saturated thiosemicarbazide for 24 h, and then immersed in a 1% silver nitrate solution for 2 d (Gallant, 1974). The stained samples were then dehydrated in an ethanol series, infiltrated with propylene oxide, and embedded in Epon. Sections of 0.1 μm thickness were mounted on copper grids previously coated with carbon and examined with a 100S transmission electron microscope (Jeol) operated at 80 keV.

Zymogram Analysis

Soluble crude extracts were prepared as previously described (Fontaine et al., 1993) and immediately stored at −70°C. The lysate was cleared by spinning at 10,000*g* for 10 min at 4°C. Proteins were measured using the Bio-Rad protein assay kit. One-hundred to 500 μg of protein in 100 μL of 25 mM Tris-Gly, pH 8.3, 1% SDS, 5% β-mercaptoethanol was denaturated by boiling in a water bath for 4 min. The denatured proteins can be stored at 4°C without subsequent loss of enzyme activity or immediately loaded on a 30:1 (acrylamide:bisacrylamide), 7.5% (0.75-mm-thick) polyacrylamide gel, run under denaturing (0.1% SDS) conditions, and containing 0.3% of rabbit liver glycogen (Sigma). Electrophoresis was carried out at room temperature at 15 V/cm for 120 min, using the Mini-Protean II cell (Bio-Rad) in 25 mM Tris-Gly, pH 8.3, 1 mM DTT, and 0.1% (w/v) SDS buffer. At the end of the run, the gel was washed twice with gentle shaking for 1 h in 100 mL of 0.04 M Tris at room temperature to remove SDS and to renaturate proteins. The gel was then incubated overnight in 50 mM glycylglycine/NaOH, pH 9.0, 100 mM $(NH_4)_2SO_4$, 15 mM β-mercaptoethanol, 5 mM $MgCl_2$, 0.5 mg/mL BSA, and 4 mM ADP-Glc at 25°C. The reaction was stopped and the gel was stained by adding 0.25% KI and 0.025% I_2. The zymogram was immediately photographed. The molecular mass of each enzyme activity detected on zymogram was measured on the same polyacrylamide gel. Some sections of the gel were stained with Coomassie blue, whereas others were renaturated and incubated as described above.

Western Blotting

Proteins of the soluble extract were separated by electrophoresis on classical SDS-PAGE gel (7.5% acrylamide and 0.1% SDS). Before blotting the proteins onto the nitrocellulose membrane (Protan BA, Schleicher & Schuell), the gels were incubated for 15 min in a western-blot buffer (48 mM

Tris, 39 mM Gly, 0.0375% [w/v] SDS, and 20% methanol). The transfer was carried out using the semidry electroblotting apparatus (Multiphor II, LKB-Pharmacia) for 45 min at 250 mA and 4°C. After incubation overnight with the specific antiserum PA55 directed against the synthetic peptide GTGGLRDTVENC, a biotin and streptavidin/alkalin phosphatase kit (Sigma) was used for immunodetection following the supplier's instructions.

RESULTS

Mutants Defective for the *STA3* Locus Lack a 115-kD Protein That Cross-Reacts with Antibodies Directed against a C-Terminal Peptide of Higher Plant Starch Synthases.

Table I summarizes the phenotypes of mutants lacking either the major GBSS, the major SSSII, or both. Although genetic evidence was sufficient to conclude that the *STA2* locus encodes the 76-kD GBSS protein (Delrue et al., 1992), the evidence that *STA3* is a structural gene for the SSSII is presently suggestive and relies on gene-dosage experiments (Fontaine et al., 1993). To characterize better the missing synthase from the *sta3* mutants, we have applied a zymogram technique that allows for denaturation of the proteins before migration and renaturation after SDS-PAGE. Comparisons of native and SDS-PAGE zymograms shown in Figures 2 and 3 were conclusive and pointed to the disappearance of a 115-kD starch synthase in all *sta3*-carrying mutants. This result was confirmed by western blotting using an antibody directed against the GTGGLRDTVENC consensus peptide sequence found in the C-terminal third of all starch synthases examined to date (Fig. 3A).

The antibody also cross-reacted with a few other proteins containing similar sequences. For instance, a strong reaction was found with a *Chlamydomonas* sp. protein homologous to acetyl-CoA acyltransferases containing the KRGGLRDTAA sequence (C. D'Hulst, personal communication). In addition, a strong cross-reaction with the 76-kD GBSS was also found when starch-bound proteins eluted from the granule were assayed by western blotting. However, to date we have found no traces of the protein in the soluble phase. Therefore, the number of cross-reacting bands displayed in Figure 3A does not reflect the number of different synthases. Only two bands of 75 and 115 kD appear in zymograms after denaturation and renaturation (Fig. 3B). A number of additional bands were detected in native gels (Fig. 2A). It is clear that all dark-staining upper bands in the zymogram disappear in the three independent *sta3* mutant alleles. The set of lighter-staining bands coeluted on the DEAE-Trisacryl anion-exchange columns (Fig. 2B) that we have previously described (Fontaine et al., 1993). In addition, this set of SSSI

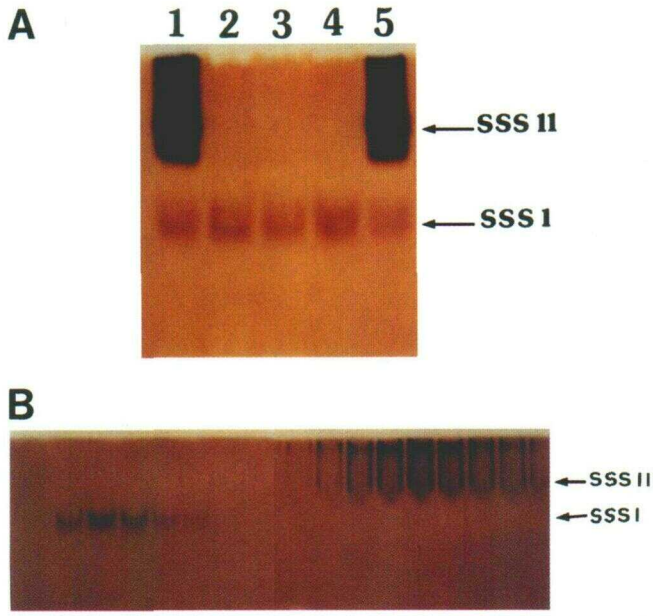

Figure 2. Starch synthase zymograms of crude and purified extracts of wild-type and mutant cells. A, One-hundred micrograms of fresh crude soluble protein extracts was subjected to native PAGE in a glycogen-containing gel. Activity staining was performed after overnight incubation in an ADP-Glc-containing buffer and stained with lugol solution (see "Materials and Methods"). Lane 1, Strain 137C (wild type); lane 2, I152 (*sta3–1*); lane 3, I154 (*sta3–2*); lane 4, I39 (*sta3–3*); lane 5, 137C (wild type). B, Five-hundred milligrams of total crude-extract protein was loaded on a DEAE-Trisacryl type M column and fed with 400 mL of 0 to 0.5 M KCl gradient as fully detailed in Fontaine et al. (1993). After dialysis 50 μL of fractions 222 to 240 (from the right to the left) was analyzed on zymograms after migration under native PAGE conditions as in A.

Table I. *Properties of starches extracted from strains defective for GBSS and SSS*

Genotype	Starch Amount[a]	Am[b]	DP_{max}[c]	Ap > 50[d]	Ap 50-22[e]	Ap 22<[f]
++	100	15–30	11	11	33	55
sta2-Δ1[g] +	100	0	11	7	39	54
+ *sta3-1*	15–40	40–60	6	26	21	53
sta2-Δ1 sta3-1	2–10	0	6	3	25	72

[a] Starch amounts are listed as relative amounts expressed as percentages of amounts accumulated by the wild-type strains after nitrogen starvation. [b] Am, Amylose weight percentage of starch measured after gel filtration of starch on Sepharose CL2B in 10 mM NaOH. [c] DP_{max} indicates degree of polymerization of the most abundant glucan in amylopectin (Ap) as measured through isoamylase debranching followed by high-performance anion exchange chromatography with pulsed amperometric detection. [d] Ap >50 indicates all Ap chains with average DP over 50. [e] Ap 50-22, Chains in which average DP are inferior to 50 and superior to 22. [f] Ap 22 <, Chains with DP under 22. The values listed are Glc weight percentages estimated by the amyloglucosidase assay with respect to the total Ap fraction. [g] *sta2-Δ1, sta2-29*::ARG7.

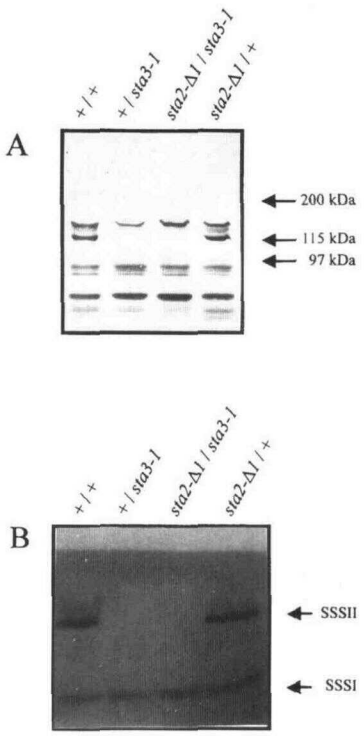

Figure 3. Western blot and starch synthase zymogram analyses of wild-type and mutant *Chlamydomonas* sp. cells. The genotypes of the strains with respect to *STA2* and *STA3* are listed above the relevant lanes. A, Western-blot analysis of soluble *Chlamydomonas* sp. proteins. Thirty micrograms of protein was loaded onto a 7.5% acrylamide gel and subjected to SDS-PAGE at 15 V/cm. B, Zymogram analysis of SSS activity. One-hundred micrograms of denatured soluble proteins was subjected to SDS-PAGE at 15 V/cm in a glycogen-containing gel (see "Materials and Methods"). After protein renaturation, the gel was further incubated overnight in an ADP-Glc-containing buffer and stained with lugol solution.

bands coeluted with a single 75-kD sharp band on our zymograms after denaturation, SDS-PAGE, and subsequent renaturation.

Under native conditions the synthases from crude or semipurified extracts never failed to give the differences in staining patterns seen in Figure 2, whereas glycogen-primed ADP-Glc incorporation assays proved that the SSSI activity amounted to 40% of the total SSS activity. This suggests that these differences in staining were due to the structure of the glycogen-primed product rather than to differences in activity amounts. Moreover, these differences vanished after denaturation-renaturation and both activities stained equally dark, suggesting interaction between SSSI and other proteins, such as branching enzymes present in the extracts both on columns and in gels. From all these experiments, we conclude that the synthase missing in strains carrying a defective *STA3* gene is a 115-kD protein.

X-Ray Diffraction of Wild-Type and Mutant Starches

In maize, most genotypes tested to date have displayed the A type of crystalline lattice (Shannon and Garwood, 1984). A noticeable exception consists of the amylose-extender high-amylose mutants that have switched to the B type. To examine the function of the three distinct synthases in the building of the amylopectin crystals, we subjected the starches extracted from either the wild-type strain 137C containing all three elongation enzymes, strain I152 of *sta3–1* genotype containing GBSSI and SSSI, strain BAFR1 carrying *sta2–29::ARG7* containing SSSI and SSSII, and strain IJ2 of *sta3–1 sta2–29::ARG7* double-mutant genotype containing SSSI only, to x-ray diffraction analysis. The diffraction diagrams obtained on the four samples are shown in Figure 4 and the corresponding relative crystallinities are listed in Table II. Both the wild type and the *sta2–29::ARG7*-carrying mutant have pure A-type crystalline structures (with diffraction peaks at 2θ values of 9.9°, 11.2°, 15°, 17°, 18.1°, and 23.3°). The crystallinities cannot be determined precisely since the water content of the different samples was impossible to adjust because of the low quantity of substrate available. Nevertheless, it is quite clear that wild type and *sta2* mutants have the highest crystallinity, respectively, of 28 and 32%. The double mutant has a lower crystallinity (20%), whereas the lowest value was found for the mutant carrying the *sta3–1* defect. In that case, the determination of the crystallinity was very tricky and did not exceed 5 to 10%. The major peak visible in the diffractogram from the *sta3–1*-carrying mutant is that of the B-type structure (classical B-type peaks are at 2θ values of 5.6°, 15°, 17°, 22°, and 24°). The double mutant displays both A- and B-type diffraction peaks and can thus be defined as a C type.

DSC

The DSC thermograms are displayed in Figure 5. The corresponding melting parameters shown in Table III are averages from three separate experiments (± 0.2°C). Wild type and mutants of the *STA2* locus exhibit a single endotherm with T_{max} at 55.3 (± 0.2°C) and 57.3°C (± 0.2°C), respectively, corresponding to starch gelatinization. The

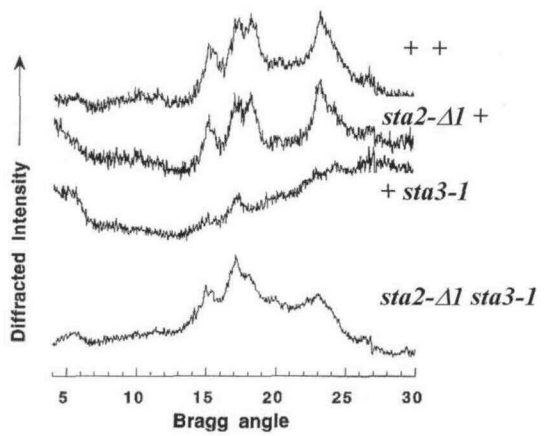

Figure 4. Wide-angle x-ray diffractograms of strains carrying various combinations of GBSS and SSS. Diffraction peaks at 2θ (Bragg angle) values of 9.9°, 11.2°, 15°, 17°, 18.1°, and 23.3° characterize the A-type starches, whereas diffraction peaks at 2θ values of 5.6°, 15°, 17°, 22°, and 24° typify B-type starches.

Table II. *Crystallinities of starches extracted from strains defective for GBSS and SSS*

Genotype	% Crystallinity	A/B[a]
++	28	
sta2-Δ1[b] +	32	
+ *sta3-1*	5–10	
sta2-Δ1 sta3-1	20	60/40

[a] A/B, Percentage of A versus B crystals in the C mixture of diffraction pattern. [b] *sta2-Δ1, sta2-29*::ARG7.

corresponding enthalpies are 8.4 (± 0.4) and 11.9 (± 0.6) J/g, respectively. This difference could be related to the slightly higher crystallinity determined for the *sta2* mutant. Moreover, the gelatinization endotherm obtained for the wild type is narrower ($T_e - T_o$ = 36.3°C), which suggests that the crystal size distribution in the wild type is more homogeneous. The two other samples yield multiple endotherms (Fig. 5) with maximum at 60°C (± 0.2°C) and 87.4°C (± 0.2°C) for the *sta3–1* mutant and at 53.3°C (± 0.2°C) and 106.3°C (± 0.2°C) for the double mutant. The first endotherms at 60 and 53.3°C correspond to starch gelatinization temperatures, and the second at a temperature ranging between 90 and 120°C is usually attributed to melting of amylose-lipid complexes formed during heating of lipid-containing starches in DSC (Biliaderis, 1992). The lipids able to be complexed by amylose are mainly fatty acids and monoglycerides (Godet et al., 1993), but the nature of the lipids present in the algal substrates studied is not well known. In the case of the *sta3–1* mutant, the second endotherm appears as a shoulder and further work is required to confirm that it is due to the melting of an amylose-lipid complex. Moreover, the double mutant contains no traces of amylose and still displays a second endotherm. The melting temperatures reported for the high amylose *sta3–1* mutant are much lower than those usually observed for high amylose maize or wrinkled pea starches (Colonna et al., 1982), which are both defective for one branching enzyme isoform. This can be related to a smaller chain length involved in the crystalline regions or a greater cooperativity in the melting process. The melting enthalpies of the *sta3–1* mutant and double-mutant starches are quite low, i.e. 3.1 and 4.2 J/g, respectively. Moreover, for the latter, the endotherm width is quite large, which probably shows a large distribution of crystal size or an independent gelatinization process for A and B types in the C mixture.

Electron Microscopy

After extraction from *C. reinhardtii* cells, the purified starch granules show somewhat the same characteristics as those displayed in vivo. Most of the wild-type starch granules are lenticular, more or less flat (Fig. 6a), and irregular in shape and size (in the range of 0.5–2.5 μm). Such irregularity in the shapes is particularly visible by transmission electron microscopy (Fig. 6b), which shows two distinct morphologies; the first group shows larger, "skullcap-like" starch granules, exceptionally up to 5 μm (probably synthesized around the pyrenoid), whereas the second group contains lenticular starch granules. Starch granules of the lenticular type are more numerous and are probably synthesized within the stroma, although further study is required for confirmation.

The starch granules of the GBSS-defective (*sta2*) mutant are smaller (0.7–1.5 μm) and have more regular shapes (Fig. 6c), similar to those of the wild-type strain. Transmission electron microscopy of *sta2* mutant granules (Fig. 6d) reveals two morphologies very close to that of smooth pea starch granules (Duprat et al., 1980), i.e. kidney and kidney-multilobed-shaped starch granules.

The starch granules of the SSSII-defective (*sta3*) mutant, which are amylose rich, show a large variety of shapes (Fig. 6, e and f) from lenticular (lens-positive) to lens-meniscus-like. A small number of starch granules are skullcap-like but they are smaller than in the wild-type strain. The size of most of the *sta3–1* starch granules varies from 0.5 to 2 μm.

The starch granules of the double mutant, which are the smallest in size (0.2–1 μm), display very distorted forms, being mostly skullcap- or ring-shaped (Fig. 6g). As reported previously (Maddelein et al., 1994), this double mutant contains numerous smaller starch granules of various, very irregular shapes and sizes (Fig. 6h).

Growth shells as seen in potato, cereals, or the legume starch granules were never found in our transmission electron microscopy experiments. However, in the same set of experiments and by using the same staining techniques, growth rings of wheat and maize starch were indeed visible and are published elsewhere (Gallant, 1974; Gallant et al., 1997). We therefore conclude that similar growth rings are absent from *Chlamydomonas* sp. starch extracted from cultures grown under continuous light and constant temperature.

DISCUSSION

Starch chromatograms on Sepharose CL-2B and TSK-HW75 and distribution of chain-lengths of debranched

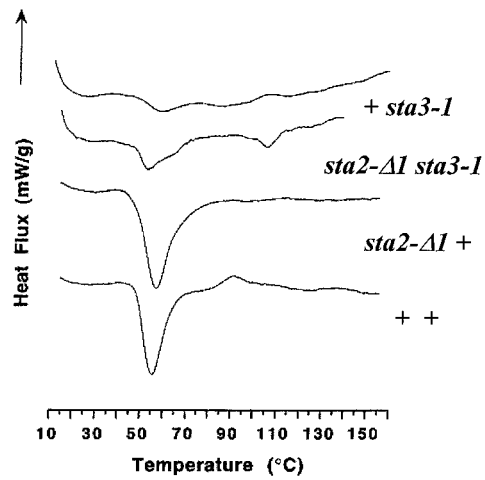

Figure 5. DSC of strains carrying various combinations of GBSS and SSS. The change in heat flux reflects the amount of energy absorbed by the sample to maintain the temperature reached by the water reference. The first endotherm, which is seen in all samples, is generally attributed to the melting of the hydrogen-bonded double-helical glucans.

Table III. *DSC of starches extracted from strains defective for GBSS and SSS*

Genotype	T_{max}	$T_e - T_o$	ΔH	T_{max}	$T_e - T_o$	ΔH
	First endotherm			Second endotherm		
	°C	°C	J/g	°C	°C	J/g
++	55.3	36.3	8.41			
sta2-Δ1[a] +	57.3	46.6	11.9			
+ sta3-1	60.1	nd[b]	3.1	87.4	nd	2.2
sta2-Δ1 sta3-1	53.3	40	4.2	106.3	24.9	1.43

[a] sta2-Δ1, sta2-29::ARG7. [b] nd, Not determined.

amylopectin could not distinguish maize endosperm starch from that of wild-type *Chlamydomonas reinhardtii* grown under nitrogen starvation (Libessart et al., 1995). We therefore suspected that the algal polysaccharide structure and composition were identical to those of maize endosperm storage starch. Indeed, many more differences in molecular weight of amylose and amylopectin chain-length distribution could be witnessed between maize and potato than between *C. reinhardtii* and maize.

In this work we take the analogy further by looking at the three-dimensional packing of glucans by wide-angle x-ray diffraction. There is no doubt that the glucans found in *C. reinhardtii* amylopectin adopt the A-crystalline lattice shown in Figure 1A. Moreover, as in maize (French, 1984) or rice (Ong et al., 1994), it is shown that it is the amylopectin fraction that is responsible for the crystallinity of starch, since mutants with no GBSS activity and consequently no amylose adopt the very same pattern and display an increase in crystallinity. The high-amylose *sta3–1* mutant with no SSSII activity has a pure B-type crystalline structure with very low crystallinity, as do most of the high-amylose starches from mutants defective for branching enzyme II (Colonna et al., 1982; Blanshard, 1987; Shi and Seib, 1995).

However, in the case of wild-type potato tuber starch and in the case of branching-enzyme-defective, high-amylose mutants, the switch to the B type was attributed to the increase in size of the unit amylopectin chains. The high-amylose *sta3–1* mutant does not contain longer amylopectin chains but, rather, accumulates both extra-short (Fontaine et al., 1993; Maddelein et al., 1994) and extra-long chains (Table I). This can be witnessed by a net decrease in T_{max} during DSC of the mutant starch, which can be due to either a decrease or shortening of the double-helical structures. This observation clearly distinguishes the SSS-defective strains from the pea and maize high-amylose, branching-enzyme-defective mutants. Moreover, the double-mutant (*sta3 sta2*) starch yields x-ray diffraction diagrams characteristic of a mixture of A- and B-type structures. The double-mutant polysaccharide was reported to have an original chain-length distribution that was shown to be intermediate between glycogen and amylopectin with a net increase in overall branching (Maddelein et al., 1994). The C type of x-ray diffraction observed together with the low melting temperature reported in DSC confirms this polysaccharide as novel and establishes that an amylopectin with a significantly lower average chain length can lead to the formation of B-type crystals in the C mixture. Our previous and present results clearly identify two SSS in *C. reinhardtii*. No evidence for a third enzyme could be found. We cannot of course exclude the presence of traces of a third enzyme. However, if present, this activity should indeed be very minor and fall below the level of detection afforded by our zymograms under native conditions. Because the absence of SSSII in *sta3* mutants leads to a decrease of over 90% in total amylopectin synthesis, we believe our results demonstrate that it is chiefly this enzyme that is responsible for the synthesis of the abundant A-type crystals in the wild-type starch of *Chlamydomonas* sp. These results further suggest that SSS are only partly redundant in function. Together with the experiments reported by Maddelein et al. (1994), they point to different contributions of these enzymes in biogenesis of the starch granule, a conclusion that we believe will hold true for higher plants.

Morphological studies of granules from *C reinhardtii* reported in this work confirm that algal starch is very small and can adopt very irregular shapes. Some of these can be attributed to the sheath of starch that surrounds the pyrenoid. Irregular shapes and small size can also be found in both transient and some storage starches from higher plants. Indeed, rice endosperm starch granules can be even smaller than those accumulated by *C. reinhardtii*. In maize the *ae* (*a*mylose *e*xtender) mutants defective for branching enzyme II synthesize starch granules with very high amylose percentages. Starch granules from *ae* mutants with an amylose content ranging between 38 and 64% were much smaller than those from normal maize (24% amylose). Mutants were characterized by numerous irregular, filamentous-shaped starch granules, and the higher the amylose content, the higher the number of abnormal starch granules (Gallant and Bouchet, 1986). Such abnormal starch granules have not been found in the high-amylose, SSSII-defective mutant, although the starch is characteristically different from the wild type.

Another interesting observation is the absence of detectable growth rings in transmission electron microscopy of sliced and stained granules. Following the work of Buttrose (1962), the growth shells of the wheat starch granules which, through structural features, are the expression of starch biosynthesis, were originally attributed to the variations in light intensity occurring during the day-night cycles. Experiments in a controlled environment (Gallant, 1974), however, have proven that the growth rings are not due to light variations but to temperature variations occurring during the day-night periods. Absence of growing shells inside the starch granules from the different strains

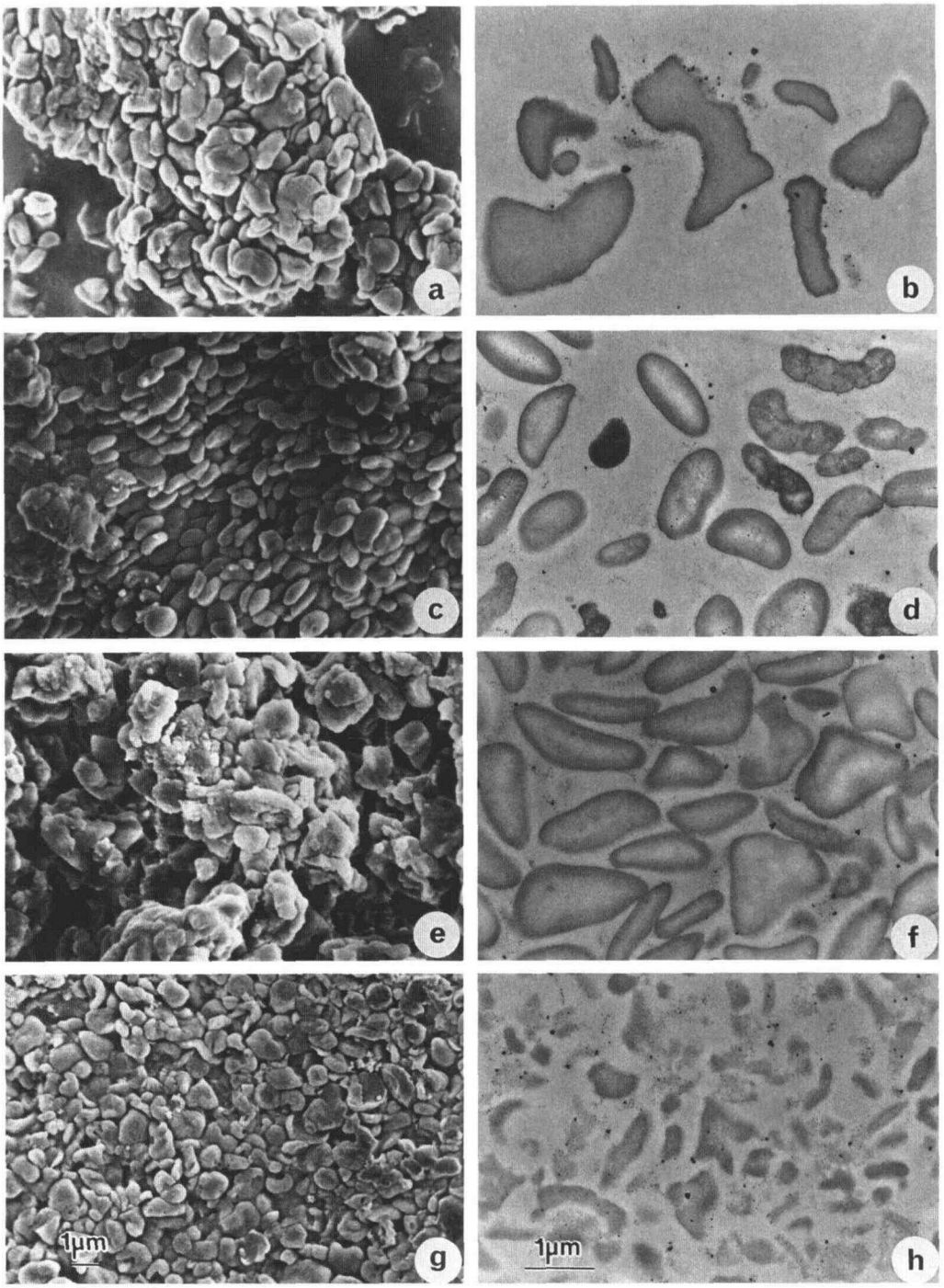

Figure 6. Electron microscopy of starches purified from mutants carrying various combinations of GBSS and SSS. a, Scanning electron microscopy of starch purified from the wild-type reference strain 137C. b, Transmission electron microscopy of sections of wild-type starch granules stained with PATAg. c, Scanning electron microscopy of starch purified from the mutant strain BAFR1 lacking GBSS activity. d, Transmission electron microscopy of sections of starch granules stained with PATAg purified from strain BAFR1 lacking GBSS activity. e, Scanning electron microscopy of starch purified from the mutant strain I152 lacking SSSII activity. f, Transmission electron microscopy of sections of starch granules stained with PATAg purified from the mutant strain I152 lacking SSSII activity. g, Scanning electron microscopy of starch purified from the mutant strain IJ2 lacking both GBSS and SSSII activities. h, Transmission electron microscopy of sections of starch granules stained with PATAg purified from the mutant strain IJ2 lacking both GBSS and SSSII activities. Bars = 1 μm.

of *Chlamydomonas* sp. cells could reflect either the stable temperature during culture or the fact that the cells were grown under continuous light. We believe that as is the case for all other aspects of starch biosynthesis and degradation, *C. reinhardtii* will prove to be an invaluable tool to study the appearance of such growth rings.

ACKNOWLEDGMENTS

The authors thank J. Davy, B. Pontoire, and A. Decq for excellent technical assistance.

Received July 28, 1997; accepted August 18, 1997.

LITERATURE CITED

Ball S, Guan H-P, James M, Myers A, Keeling P, Mouille G, Buléon A, Colonna P, Preiss J (1996) From glycogen to amylopectin: a model explaining the biogenesis of the plant starch granule. Cell **86:** 349–352

Ball S, Marianne T, Dirick L, Fresnoy M, Delrue B, Decq A (1991) A *Chlamydomonas reinhardtii* low-starch mutant is defective for 3-phosphoglycerate activation and orthophosphate inhibition of ADP-glucose pyrophosphorylase. Planta **185:** 17–26

Ball SG, Dirick L, Decq A, Martiat JC, Matagne RF (1990) Physiology of starch storage in the monocellular alga *Chlamydomonas reinhardtii*. Plant Sci **66:** 1–9

Biliaderis CG (1992) Structures and phase transitions of starch in food systems. Food Technol **6:** 98–109

Blanshard JMV (1987) Starch granule structure and function. *In* T Gaillard, ed, Crit Rev App Chem, Vol 13. John Wiley & Sons, pp 16–54

Buttrose MS (1962) The influence of environment on the shell structure of the starch granule. J Cell Biol **14:** 159–167

Colonna P, Buléon A, Mercier C, Lemaguer M (1982) *Pisum sativum* and *Vicia faba* carbohydrates. IV. Granular structure of wrinkled pea starch. Carbohyd Polym **2:** 43

Delrue B, Fontaine, T, Routier F, Decq A, Wieruszeski JM, Van Den Koornhuyse N, Maddelein ML, Fournet B, Ball S (1992) Waxy *Chlamydomonas reinhardtii*: monocellular algal mutants defective in amylose biosynthesis and granule-bound starch synthase activity accumulate a structurally modified amylopectin. J Bacteriol **174:** 3612–3620

Duprat F, Gallant DJ, Guilbot A, Mercier C, Robin J-P (1980) L'amidon. *In* B Monties, ed, Les polymères végétaux. Gauthier-Villars, Paris, pp 176–229

Fontaine T, D'Hulst C, Maddelein M-L, Routier F, Marianne-Pepin T, Decq A, Wieruszeski JM, Delrue B, Van Den Koornhuyse N, Bossu J-P, and others (1993) Toward an understanding of the biogenesis of the starch granule: evidence that *Chlamydomonas* soluble starch starch synthase II controls the synthesis of intermediate size glucans of amylopectin. J Biol Chem **268:** 16223–16230

French D (1984) Organization of starch granules. *In* RL Whistler, JN Bemiller, EF Parschall, eds, Starch, Chemistry and Technology. Academic Press, New York, pp 183–247

Gallant DJ (1974) Contribution à l'étude de la structure et de l'ultrastructure du grain d'amidon. PhD thesis, University of Paris Centre National de la Recherche Scientifique no. AO 10823

Gallant DJ, Bouchet B (1986) Ultrastructure of maize starch granules: a review. J Food Microstruct **5:** 141–155

Gallant DJ, Bouchet B, Baldwin P (1997) Microscopy of starch: evidence for a new level of granule organization. Carbohyd Polym **32:** 177–191

Godet MC, Tran V, Delage MM, Buléon A (1993) Molecular modelling of the specific interactions involved in the amylose complexation by fatty acids. Int J Biol Macromol **15:** 11–16

Harris EH (1989a) Culture and storage methods. *In* E Harris, ed, The *Chlamydomonas* Sourcebook. A Comprehensive Guide to Biology and Laboratory Use. Academic Press, San Diego, CA, pp 25–63

Harris EH (1989b) Genetic analysis. *In* E Harris, ed, The *Chlamydomonas* Sourcebook. A Comprehensive Guide to Biology and Laboratory Use. Academic Press, San Diego, CA, pp 399–446

Imberty A, Buléon A, Tran V Pérez S (1991) Recent advances in knowledge of starch structure. Starch/Stärke **43:** 375–384

Imberty A, Chanzy H, Pérez S, Buléon A, Tran V (1988) The double-helical nature of the crystalline part of A-starch. J Mol Biol **20:** 2634–2636

Imberty A, Pérez S (1988) A revisit to the three-dimensional structure of β-amylose. Biopolymers **27:** 1205–1221

Libessart N, Maddelein M-L, Van Den Koornhuyse N, Decq A, Delrue B, Mouille G, D'Hulst C, Ball SG (1995) Storage, photosynthesis and growth: the conditional nature of mutations affecting starch synthesis and structure in *Chlamydomonas reinhardtii*. Plant Cell **7:** 1117–1127

Maddelein M-L, Libessart N, Bellanger F, Delrue B, D'Hulst C, Van Den Koornhuyse N, Fontaine T,Wieruszeski JM, Decq A, Ball SG (1994) Toward an understanding of the biogenesis of the starch granule: determination of granule-bound and soluble starch synthase functions in amylopectin synthesis. J Biol Chem **269:** 25150–25157

Mouille G, Maddelein M-L, Libessart N, Talaga P, Decq A, Delrue B, Ball S (1996) Phytoglycogen processing: a mandatory step for starch biosynthesis in plants. Plant Cell **8:** 1353–1366

Müller-Röber B, Kossmann J (1994) Approaches to influence starch quantity and starch quality in transgenic plants. Plant Cell Environ **17:** 601–613

Murthy NS, Minor H (1990) General procedure for evaluating amorphous scattering and crystallinity from x-ray diffraction scans of semicrystalline polymers. Polymer **31:** 996–1002

Ong MH, Julek K, Tokarczuk PF, Blanshard JM, Harding SE (1994) Simultaneous determinations of the molecular weight distributions of amyloses and the fine structures of amylopectins of native starches. Carbohydr Res **260:** 83–98

Preiss J, Sivak MN (1996) Starch synthesis in sinks and sources. *In* E Zamski, A Schaffer, Eds, Photoassimilate Distribution in Plants and Crops: Source-Sink Relationships. Marcel Dekker, New York, pp 63–96

Shannon JC, Garwood DL (1984) Genetics and physiology of starch development. *In* RL Whistler, JN Bemiller, EF Paschall, eds, Starch: Chemistry and Technology, Ed 2. Academic Press, Orlando, FL, pp 25–86

Shi YC, Seib PA (1995) Fine structure of maize starches from four wx-containing genotypes of the W64A inbred line in relation to gelatinization and retrogradation. Carbohydr Polym **26:** 141–147

Smith AM, Denyer K, Martin C (1997) The synthesis of the starch granule. Annu Rev Plant Physiol Plant Mol Biol **48:** 67–87

Van den Koornhuyse N, Libessart N, Delrue B, Zabawinski C, Decq A, Iglesias A, Preiss J, Ball, S (1996) Control of starch composition and structure through substrate supply in the monocellular alga *Chlamydomonas reinhardtii*. J Biol Chem **271:** 16281–16288